

V

Charged leptons

From the viewpoint of probing the basic structure of the Standard Model, the charged leptons constitute an attractive starting point. Since effects of the strong interaction are generally either absent or else play a secondary role, the theoretical analysis is relatively clean. Moreover, a great deal of high-quality data has been amassed involving these particles. Thus, charged leptons serve as an ideal system for defining our renormalization prescription, and for investigating the effects of various radiative corrections.

V-1 The electron

Some of the most precise tests of the Standard Model (or more exactly of *QED*) occur within the elementary electron–proton system. The renormalization program for the theory has been introduced in Sect. II-1, where it was shown how ultraviolet divergent contributions to such calculations can be removed by means of subtraction from a finite number of suitably constructed counterterms. Here we examine the finite pieces which remain after such subtractions and compare theory with experiment.

Breit–Fermi interaction

The electromagnetic properties of the electron are studied by use of a photon probe. To lowest order, the $\bar{e}\gamma$ vertex has the structure

$$\langle e(\mathbf{p}'_e, \lambda'_e) | J_{\text{em}}^\mu | e(\mathbf{p}_e, \lambda_e) \rangle = -e \bar{u}(\mathbf{p}'_e, \lambda'_e) \gamma^\mu u(\mathbf{p}_e, \lambda_e), \quad (1.1)$$

and the interaction between two charged particles is governed by the exchange of a single virtual photon. An important example is the electron–proton interaction, which has the invariant amplitude¹

¹ We work temporarily with an ‘ideal’ proton – a point particle having no anomalous magnetic moment.

$$\mathcal{M}_{eP} = e^2 \bar{u}(\mathbf{p}'_e, \lambda'_e) \gamma^\mu u(\mathbf{p}_e, \lambda_e) \frac{1}{q^2} \bar{u}(\mathbf{p}'_p, \lambda'_p) \gamma_\mu u(\mathbf{p}_p, \lambda_p), \tag{1.2}$$

where $\mathbf{p}_e, \mathbf{p}'_e$ and $\mathbf{p}_p, \mathbf{p}'_p$ are respectively electron and proton momenta and $q = p_e - p'_e$ is the four-momentum transfer. In the following, we shall demonstrate how the above single-photon exchange amplitude is associated with well-known contributions in atomic physics. Denoting proton two-spinors with tildes, we begin by reducing the amplitude of Eq. (1.2) in the small-momentum limit to

$$\begin{aligned} \mathcal{M}_{eP} \simeq & -\frac{e^2}{\mathbf{q}^2} \left[1 - \frac{\mathbf{p}_e^2 + \mathbf{p}'_e{}^2}{8m_e^2} \right] \left[1 - \frac{\mathbf{p}_p^2 + \mathbf{p}'_p{}^2}{8m_p^2} \right] \\ & \times \left[\tilde{\chi}^{\prime\dagger} \left[1 + \frac{\mathbf{p}'_p \cdot \mathbf{p}_p + i\boldsymbol{\sigma} \cdot \mathbf{p}'_p \times \mathbf{p}_p}{4m_p^2} \right] \tilde{\chi} \chi^{\prime\dagger} \left[1 + \frac{\mathbf{p}'_e \cdot \mathbf{p}_e + i\boldsymbol{\sigma} \cdot \mathbf{p}'_e \times \mathbf{p}_e}{4m_e^2} \right] \chi \right. \\ & \left. - \tilde{\chi}^{\prime\dagger} \frac{\mathbf{p}_p + \mathbf{p}'_p - i\boldsymbol{\sigma} \times (\mathbf{p}_p - \mathbf{p}'_p)}{2m_p} \tilde{\chi} \cdot \chi^{\prime\dagger} \frac{\mathbf{p}_e + \mathbf{p}'_e - i\boldsymbol{\sigma} \times (\mathbf{p}_e - \mathbf{p}'_e)}{2m_e} \chi \right], \tag{1.3} \end{aligned}$$

where m_e, m_p are, respectively, the electron and proton masses. The various terms in the above expression can be interpreted physically by recalling that in Born approximation the transition amplitude and interaction potential are Fourier transforms of each other,

$$V_{eP}(\mathbf{r}) = \int \frac{d^3q}{(2\pi)^3} e^{-i\mathbf{q}\cdot\mathbf{r}} \mathcal{M}_{eP}, \tag{1.4}$$

where $\mathbf{r} = \mathbf{r}_e - \mathbf{r}_p$. From the relation

$$\int \frac{d^3q}{(2\pi)^3} e^{-i\mathbf{q}\cdot\mathbf{r}} \frac{1}{\mathbf{q}^2} = \frac{1}{4\pi r}, \tag{1.5}$$

we recognize the leading (velocity-independent) term,

$$V_{\text{Coul}} = -\frac{e^2}{4\pi r} \tilde{\chi}^{\prime\dagger} \tilde{\chi} \chi^{\prime\dagger} \chi, \tag{1.6}$$

as the Coulomb interaction between electron and proton. The identity

$$-\int \frac{d^3q}{(2\pi)^3} \frac{e^2}{\mathbf{q}^2} \frac{i\boldsymbol{\sigma} \cdot \mathbf{p}'_e \times \mathbf{p}_e}{4m_e^2} e^{-i\mathbf{q}\cdot\mathbf{r}} = \frac{e^2}{4m_e^2} \frac{\boldsymbol{\sigma} \cdot \mathbf{r} \times \mathbf{p}_e}{4\pi r^3} \tag{1.7}$$

allows us to recognize an additional piece of Eq. (1.3) as the spin-orbit potential, which is often expressed as

$$V_{s-o} = \frac{1}{2m_e^2} \frac{1}{r} \frac{dV_0}{dr} \tilde{\chi}^{\prime\dagger} \tilde{\chi} \chi^{\prime\dagger} \frac{\boldsymbol{\sigma}}{2} \cdot \mathbf{r} \times \mathbf{p}_e \chi, \tag{1.8}$$

but evaluated in this instance with $V_0 = -e^2/4\pi r$. Combining the remaining $\mathcal{O}(\mathbf{p}^2/m_e^2)$ terms in Eq. (1.3), we can cancel the \mathbf{q}^2 term in the denominator to obtain the so-called Darwin potential,

$$V_D = \frac{e^2}{8m_e^2} \delta^{(3)}(r) \tilde{\chi}'^\dagger \tilde{\chi} \chi'^\dagger \chi. \quad (1.9)$$

This term has its origin in the electric interaction between the particles, and by employing the Gauss' law relation,

$$\nabla \cdot \mathbf{E}_{\text{Coul}} = e\delta^{(3)}(r), \quad (1.10)$$

it can be re-expressed in the equivalent form

$$V_D = \frac{e}{8m_e^2} \nabla \cdot \mathbf{E}_{\text{Coul}} \tilde{\chi}'^\dagger \tilde{\chi} \chi'^\dagger \chi. \quad (1.11)$$

The spin-orbit and Darwin potentials, together with the $\mathcal{O}(\mathbf{p}^2/m_e^2)$ relativistic corrections to the electron kinetic energy, give rise to atomic *fine structure* energy effects.

The remaining terms in the photon exchange interaction of Eq. (1.3) are effects produced by electron and proton current densities, the terms $(\mathbf{p}_e + \mathbf{p}'_e)/2m_e$ and $-i\boldsymbol{\sigma} \times (\mathbf{p}_e - \mathbf{p}'_e)/2m_e$ representing convection and magnetization contributions, respectively. In particular, the interaction between magnetization densities is equivalent to the dipole-dipole potential

$$V_{\text{dple-dple}} = -\frac{e}{m_e} \chi'^\dagger \frac{\boldsymbol{\sigma}}{2} \chi \cdot \nabla \times \left(\frac{e}{m_p} \tilde{\chi}'^\dagger \frac{\boldsymbol{\sigma}}{2} \tilde{\chi} \times \nabla \frac{1}{4\pi r} \right). \quad (1.12)$$

Recognizing that the magnetic field produced by the magnetic dipole moment of a (point) proton is

$$\mathbf{B}_{\text{proton}} = \nabla \times \left(\frac{e}{m_p} \tilde{\chi}'^\dagger \frac{\boldsymbol{\sigma}}{2} \tilde{\chi} \times \nabla \frac{1}{4\pi r} \right), \quad (1.13)$$

we can interpret the hyperfine energy as the interaction between the electron magnetic moment and the spin-induced proton magnetic field. Upon dropping the proton and electron spinors and using the identity

$$\nabla_i \nabla_j \frac{1}{r} = 3 \frac{x_i x_j}{r^5} - \delta_{ij} \left[\frac{1}{r^3} + \frac{4\pi}{3} \delta^{(3)}(\mathbf{r}) \right], \quad (1.14)$$

the dipole-dipole interaction may be written as a sum of *hyperfine* and *tensor* terms,

Table V-1. Precision tests of QED.

	Experiment	Theory
ν_{hyp}^b	1420.405 751 767(1)	1420.403(1)
a_e^a	1159.65218076(27)	1159.65218178(77)
a_μ^a	1165.92089(54)(33)	1165.91802(2)(42)(26)
$\Delta E_{n=2}^{(\text{Lamb})b}$	1057845.0(9.0)	1057844.4(1.8)

$a \times 10^{-6}$

b In units of kHz.

$$\begin{aligned}
 V_{\text{dple-dple}} &= V_{\text{hyp}} + V_{\text{tensor}}, \\
 V_{\text{hyp}} &= \frac{8\pi\alpha}{3m_e m_p} \mathbf{s}_e \cdot \mathbf{s}_p \delta^{(3)}(\mathbf{r}), \\
 V_{\text{tensor}} &= \frac{\alpha}{m_e m_p r^3} [3(\mathbf{s}_e \cdot \hat{\mathbf{r}})(\mathbf{s}_p \cdot \hat{\mathbf{r}}) - \mathbf{s}_e \cdot \mathbf{s}_p].
 \end{aligned}
 \tag{1.15}$$

Denoting the total electron-proton spin as $\mathbf{s}_{\text{tot}} = \mathbf{s}_e + \mathbf{s}_p$, it follows that the hyperfine interaction splits the hydrogen atom ground state into components with $s_{\text{tot}} = 1$ and $s_{\text{tot}} = 0$. The frequency associated with this splitting is one of the most precisely measured constants in physics and is the source of the famous 21-cm radiation of radioastronomy. As seen in Table V-1, the experimental determination is about six orders of magnitude more precise than the theoretical value. Precision in the latter is limited by the nuclear force contribution (about 3 parts in 10^5).

Let us gather all the terms discussed thus far. In addition, we treat the proton and electron on an equal footing, since it will prove instructive when we discuss models of quark interactions in Chaps. XI-XIII. We then obtain the full one-photon exchange potential (Breit-Fermi interaction) for the electron-proton system,

$$\begin{aligned}
 V_{\text{one-photon}} &= -\frac{\alpha}{r} + \frac{8\pi\alpha}{3m_e m_p} \delta^{(3)}(\mathbf{r}) \mathbf{s}_e \cdot \mathbf{s}_p + \frac{\pi\alpha}{2} \delta^{(3)}(\mathbf{r}) \left[\frac{1}{m_e^2} + \frac{1}{m_p^2} \right] \\
 &+ \frac{\alpha}{m_e m_p r^3} [3(\mathbf{s}_e \cdot \hat{\mathbf{r}})(\mathbf{s}_p \cdot \hat{\mathbf{r}}) - \mathbf{s}_e \cdot \mathbf{s}_p] \\
 &+ \frac{\alpha}{r^3} \left[\frac{\mathbf{s}_e \cdot \mathbf{r} \times \mathbf{p}_e}{2m_e^2} - \frac{\mathbf{s}_p \cdot \mathbf{r} \times \mathbf{p}_p}{2m_p^2} + \frac{\mathbf{s}_p \cdot \mathbf{r} \times \mathbf{p}_e - \mathbf{s}_e \cdot \mathbf{r} \times \mathbf{p}_p}{m_e m_p} \right] \\
 &+ \frac{\alpha}{2m_e m_p r} [\mathbf{p}_e \cdot \mathbf{p}_p + \hat{\mathbf{r}}(\hat{\mathbf{r}} \cdot \mathbf{p}_e) \cdot \mathbf{p}_p],
 \end{aligned}
 \tag{1.16}$$

where we recall $\mathbf{r} \equiv \mathbf{r}_e - \mathbf{r}_p$ and note that a spin-independent *orbit-orbit* interaction has been included as the final term. The single-photon exchange interaction is

seen to include a remarkable range of effects, all of which are necessary to understand details of atomic spectra.

QED corrections

Also important in precision tests of atomic systems are the higher order *QED* corrections. We have just demonstrated how the simple q^2 piece of the photon propagator leads to the Breit–Fermi interaction between electron and proton. The vacuum polarization correction discussed in Sect. II–1 produces an additional component of the e – P interaction called the *Uehling* potential. From Eq. (II–1.37), we recall that in the on-shell renormalization scheme the subtracted vacuum polarization $\bar{\Pi}$ behaves in the small-momentum limit $m_e^2 \gg q^2$ as

$$\bar{\Pi}(q) = \frac{e^2}{60\pi^2} \frac{q^2}{m_e^2} + \mathcal{O}\left(\frac{q^4}{m_e^4}\right).$$

By the process of Fig. II–3, this yields the contribution

$$V_{\text{Uehling}}(r) = \int \frac{d^3q}{(2\pi)^3} e^{-i\mathbf{q}\cdot\mathbf{r}} \frac{e^2}{q^2} \times \frac{e^2}{60\pi^2} \frac{q^2}{m_e^2} = \frac{4}{15} \frac{\alpha^2}{m_e^2} \delta^{(3)}(\mathbf{r}). \quad (1.17)$$

The presence of the delta function implies that S -wave states of the hydrogen atom are shifted by this potential while other partial waves are not. Contributions from the Uehling potential have been observed in scattering experiments despite its $\mathcal{O}(\alpha)$ suppression relative to the dominant Coulomb scattering [Ve *et al.* 89].

The photon–electron vertex is also affected by radiative corrections. Let us write the proper ($1PI$) electron–photon vertex through first order in α as

$$ie\Gamma_v(p'_e, p_e) = ie\gamma_v + ie\Lambda_v(p'_e, p_e) + \dots, \quad (1.18)$$

where, referring to Fig. II–2(b), we have in Feynman gauge

$$ie\Lambda_v(p'_e, p_e) = (ie)^3 \int \frac{d^4k}{(2\pi)^4} \frac{-ig^{\alpha\beta}}{k^2 - \lambda^2 + i\epsilon} \\ \times \gamma_\alpha \frac{i}{\not{p}'_e - \not{k} - m_e + i\epsilon} \gamma_v \frac{i}{\not{p}_e - \not{k} - m_e + i\epsilon} \gamma_\beta. \quad (1.19)$$

Note that a small photon mass λ has been inserted to act as a cut-off in the small-momentum domain, and we take both incoming and outgoing electrons to obey $p_e^2 = p_e'^2 = m_e^2$. With a modest effort, the integral in Eq. (1.19) can be continued to d spacetime dimensions,

$$ie\Lambda_\nu(p'_e, p_e) = (ie)^3 i\mu^{2\epsilon} \int_0^1 dx \int \frac{d^d k}{(2\pi)^d} \times \frac{(2\epsilon - 2)\not{k}\gamma_\nu\not{k} + 4\not{k}(p_e + p'_e)_\nu - 4m_e k_\nu - 4(p_e + p'_e) \cdot k\gamma_\nu + 4p_e \cdot p'_e\gamma_\nu}{[k^2 - \lambda^2 + i\epsilon][(k - p_x)^2 - p_x^2 + i\epsilon]^2}, \tag{1.20}$$

where $p_x \equiv xp_e + (1 - x)p'_e$, and the result of performing the k -integration can be expressed as

$$ie\Lambda_\nu(p'_e, p_e) = (I_1)_\nu + (I_2)_\nu, \tag{1.21}$$

where $(I_1)_\nu$ is singular in the $\epsilon \rightarrow 0$ limit,

$$(I_1)_\nu = i\gamma_\nu \frac{e^3}{(4\pi)^2} \frac{\Gamma(\epsilon)}{(4\pi)^{-\epsilon}} \frac{(2\epsilon - 2)^2 \mu^{2\epsilon}}{2} \int_0^1 dx \int_0^1 dy \frac{y}{[y^2 p_x^2 + \lambda^2(1 - y)]^\epsilon}, \tag{1.22}$$

and $(I_2)_\nu$ is not,

$$(I_2)_\nu = i \frac{e^3}{(4\pi)^2} \frac{\mu^{2\epsilon} \Gamma(1 + \epsilon)}{(4\pi)^{-\epsilon}} \int_0^1 dx \int_0^1 dy \frac{N_\nu}{[y^2 p_x^2 + \lambda^2(1 - y)]^{\epsilon+1}}$$

$$N_\nu = y^3(2\epsilon - 2)\not{p}_x\gamma_\nu\not{p}_x + 4y^2[(p_e + p'_e)_\nu\not{p}_x - m_e(p_x)_\nu - (p_e + p'_e) \cdot p_x\gamma_\nu] + 4yp_e \cdot p'_e\gamma_\nu. \tag{1.23}$$

The singular term $(I_1)_\nu$, which arises from the $\not{k}\gamma_\nu\not{k}$ term in Eq. (1.20), is infrared-finite, and thus the photon mass λ can be dropped from it. Upon expanding $(I_1)_\nu$ in powers of ϵ and performing the y -integral, we obtain

$$(I_1)_\nu = ie\gamma_\nu \frac{e^2}{16\pi^2} \left[\frac{1}{\epsilon} + \ln(4\pi) - \gamma - 1 - \int_0^1 dx \ln\left(\frac{p_x^2}{\mu^2}\right) + \mathcal{O}(\epsilon) \right]. \tag{1.24}$$

Because $(I_2)_\nu$ is not multiplied by any quantity which is singular in ϵ , we can immediately take the $\epsilon \rightarrow 0$ limit to cast it in the form

$$(I_2)_\nu = -i \frac{e^3}{16\pi^2} \int_0^1 dx \int_0^1 dy \frac{N_\nu}{y^2 p_x^2 + \lambda^2(1 - y)},$$

$$N_\nu = -2y^3\not{p}_x\gamma_\nu\not{p}_x + 4yp_e \cdot p'_e\gamma_\nu + 4y^2[(p_e + p'_e)_\nu\not{p}_x - m_e(p_x)_\nu - (p_e + p'_e) \cdot p_x\gamma_\nu]. \tag{1.25}$$

The photon mass λ can be dropped from the terms in N_ν proportional to y^2 and y^3 since they are nonsingular even if $\lambda = 0$. Performing the y -integration then yields the result,

$$(I_2)_v = -i \frac{e^3}{16\pi^2} \int_0^1 dx p_x^{-2} (-\not{p}_x \gamma_\nu \not{p}_x + 2p_e \cdot p'_e \gamma_\nu \ln(p_x^2/\lambda^2) + 4 [(p_e + p'_e)_\nu \not{p}_x - m_e(p_x)_\nu - (p_e + p'_e) \cdot p_x \gamma_\nu]). \tag{1.26}$$

The identities

$$\not{p}_x \gamma_\nu \not{p}_x = 2m_e(p_x)_\nu - p_x^2 \gamma_\nu, \quad (p_e + p'_e) \cdot p_x = 2m_e^2 - q^2/2, \tag{1.27}$$

$$p_x^2 = m_e^2 - q^2 x(1-x)$$

allow $(I_2)_v$ to be expressed in terms of $q^2 = (p_e - p'_e)^2$, and the dependence of p_x^2 on the symmetric combination $x(1-x)$ implies

$$\int_0^1 dx (p_x)_\nu f(p_x^2) = \frac{1}{2} (p_e + p'_e)_\nu \int_0^1 dx f(p_x^2). \tag{1.28}$$

These steps, plus use of the Gordon decomposition of Eq. (C-2.8) finally lead to the expression

$$ie\Gamma_\nu(p'_e, p_e) = ie\gamma_\nu \left[1 + \frac{e^2}{4\pi^2} \left\{ \frac{1}{4\epsilon} - \frac{2 + \gamma - \ln(4\pi)}{4} - \frac{1}{4} \int_0^1 dx \ln \left(\frac{m_e^2 - q^2 x(1-x)}{\mu^2} \right) + \frac{1}{2} \int_0^1 dx \frac{3m_e^2 - q^2}{m_e^2 - q^2 x(1-x)} - \frac{2m_e^2 - q^2}{4} \int_0^1 dx \frac{1}{m_e^2 - q^2 x(1-x)} \ln \left(\frac{m_e^2 - q^2 x(1-x)}{\lambda^2} \right) \right\} \right] - ie \left[-\frac{i\sigma_{\nu\beta} q^\beta}{2m_e} \frac{e^2}{8\pi^2} \int_0^1 dx \frac{m_e^2}{m_e^2 - q^2 x(1-x)} \right]. \tag{1.29}$$

In the on-shell renormalization program, the electron-photon vertex

$$ie\Gamma_\nu^{(o-s)}(p'_e, p_e) \equiv ieZ_1^{(o-s)}\Gamma_\nu(p'_e, p_e) \tag{1.30}$$

is constrained to obey

$$\lim_{q \rightarrow 0} ie\Gamma_\nu^{(o-s)}(p'_e, p_e) = ie\gamma_\nu, \tag{1.31}$$

so that

$$Z_1^{(o-s)} = 1 - \frac{e^2}{4\pi^2} \left[\frac{1}{4\epsilon} + 1 - \frac{\gamma - \ln(4\pi)}{4} - \frac{1}{4} \ln \left(\frac{m_e^2}{\mu^2} \right) - \frac{1}{2} \ln \left(\frac{m_e^2}{\lambda^2} \right) \right] = Z_1^{(MS)} - \frac{e^2}{4\pi^2} \left[1 - \frac{\gamma - \ln(4\pi)}{4} - \frac{1}{4} \ln \left(\frac{m_e^2}{\mu^2} \right) - \frac{1}{2} \ln \left(\frac{m_e^2}{\lambda^2} \right) \right]. \tag{1.32}$$

The on-shell renormalized vertex is thus given by

$$ie\Gamma_\nu^{(o-s)}(p'_e, p_e) = ie \left(\gamma_\nu F_1(q^2) - \frac{i\sigma_{\nu\beta} q^\beta}{2m_e} F_2(q^2) \right), \tag{1.33}$$

where $F_1(q^2)$ is given by a complicated expression which we do not reproduce here, and

$$F_2(q^2) = \frac{e^2}{8\pi^2} \int_0^1 dx \frac{m_e^2}{m_e^2 - q^2x(1-x)}. \tag{1.34}$$

In addition to its original spin structure γ_ν , the electromagnetic vertex is seen in Eq. (1.33) to have picked up a contribution proportional to $\sigma_{\nu\beta}q^\beta$. The γ_ν and $\sigma_{\nu\beta}q^\beta$ contributions are called the *Dirac* and *Pauli* terms respectively, and $F_1(q^2)$ and $F_2(q^2)$ are the Dirac and Pauli *form factors* of the electron. The vertex correction turns out to have several important experimental consequences.

Consider the interaction of an electron with a classical electromagnetic field for very small q^2 . Using Eq. (1.33) and the Gordon identity, we have

$$\begin{aligned} \mathcal{H}_{\text{int}} &= eA_\nu(x)\langle e(\mathbf{p}'_e)|J_{\text{em}}^\nu(x)|e(\mathbf{p}_e)\rangle \\ &= -eA_\nu(x)\bar{u}(\mathbf{p}'_e)\left[\gamma^\nu - \frac{i\sigma^{\nu\beta}q_\beta}{2m_e}\frac{e^2}{8\pi^2}\right]u(\mathbf{p}_e)e^{-iq\cdot x} + \mathcal{O}(q^2) \\ &= -eA_\nu(x)\bar{u}(\mathbf{p}'_e)\left[\frac{(p_e + p'_e)^\nu}{2m_e} - \frac{i\sigma^{\nu\beta}q_\beta}{2m_e}\left(1 + \frac{e^2}{8\pi^2}\right)\right]u(\mathbf{p}_e)e^{-iq\cdot x} + \mathcal{O}(q^2). \end{aligned} \tag{1.35}$$

Precision tests of QED

Some of the most severe tests of the Standard Model have come from comparing theory and experiment in ever more precise determinations of electromagnetic particle properties [MoNT 12]. Among these, the topic of lepton magnetic moments has achieved a deserved prominence, and we turn to this now by continuing the discussion of the previous section.

The first term in Eq. (1.35) describes the coupling of the photon to the convective current of electron, but it is the second term which interests us here. Ignoring the convective term and integrating by parts, we obtain to lowest order in q ,

$$\begin{aligned} eA_\nu(x)\langle p'_e|J_{\text{em}}^\nu(x)|p_e\rangle &= -e\bar{u}(p'_e)\frac{\sigma^{\beta\nu}\partial_\beta A_\nu(x)}{2m_e}\left(1 + \frac{e^2}{8\pi^2}\right)u(p_e)e^{-iq\cdot x} \\ &= -e\bar{u}(p'_e)\frac{\sigma^{\beta\nu}F_{\beta\nu}(x)}{4m_e}\left(1 + \frac{e^2}{8\pi^2}\right)u(p_e)e^{-iq\cdot x}. \end{aligned} \tag{1.36}$$

Noting that in the nonrelativistic limit $\sigma^{\beta\nu}F_{\beta\nu}/2 \rightarrow -\boldsymbol{\sigma} \cdot \mathbf{B}$, we see that this is the coupling of a magnetic field to the electron magnetic moment. The result is usually expressed in terms of the gyromagnetic ratio g_{el} , where $\boldsymbol{\mu}_e \equiv -eg_{\text{el}}\mathbf{s}_e/2m_e$, and to order e^2 we have

$$a_e \equiv \frac{g_{el} - 2}{2} = \frac{\alpha}{2\pi} + \mathcal{O}\left(\frac{\alpha^2}{\pi^2}\right) \simeq 0.00116\dots \tag{1.37}$$

Clearly, the radiative corrections have modified the Dirac equation value, $g_{el}^{(\text{Dirac})} = 2$. The factor $\alpha/2\pi$, which arises from the Pauli term, is but the first of the anomalous *QED* contributions.

For definiteness, let us now focus on theoretical corrections to the *muon* magnetic moment.² The *QED* component, whose first nontrivial term is shown in Eq. (1.37), encompasses Feynman diagrams with multiple photon exchanges as well as charged lepton loops. It is expressible as a series in powers of α/π ,

$$a_\mu^{(\text{QED})} = \frac{\alpha}{2\pi} + 0.765857410(27) \left(\frac{\alpha}{\pi}\right)^2 + \dots \tag{1.38a}$$

Contributions through $(\alpha/\pi)^5$ have, in fact, been calculated.

There is a smaller electroweak (EW) sector with diagrams comprising virtual W^\pm , Z^0 and Higgs-boson exchanges. The leading order term is given by

$$a_\mu^{(\text{EW})} = \frac{G_\mu m_\mu^2}{8\sqrt{2}\pi^2} \left[\frac{5}{3} + \frac{1}{3} (1 - 4 \sin^2 \theta_w)^2 + \mathcal{O}\left(\frac{m_\mu^2}{M_W^2}\right) + \mathcal{O}\left(\frac{m_\mu^2}{M_H^2}\right) + \dots \right], \tag{1.38b}$$

where G_μ and θ_w are respectively the muon decay constant and the Weinberg angle. We will discuss each of these later, G_μ in Sect. V–2 and θ_w in Sect. XVI–2.

Finally, there are important corrections from the strong interactions. It can be shown that these are largely influenced by effects of relatively low-energy hadronic physics. For example, at the *QCD* level the lowest order correction amounts to a quark–antiquark vacuum polarization, expressible in terms of either e^+e^- cross sections or vector spectral functions from τ decay (see Sect. V–3),

$$\begin{aligned} a_\mu^{(\text{Had})}[\text{LO}] \times 10^{11} &= 6\,923(42)(3) \quad [\sigma(e^+e^- \rightarrow \text{hadrons})] \\ &= 7\,015(42)(19)(3) \quad [\tau \text{ decay}]. \end{aligned}$$

Upon using the e^+e^- cross-section data, one finds for the total,

$$\begin{aligned} a_\mu^{(\text{SM})} &= a_\mu^{(\text{QED})} + a_\mu^{(\text{EW})} + a_\mu^{(\text{Had})} \\ &= [116\,584\,718.09(0.15) + 154.(1)(2) + 6\,923(42)(3)] \times 10^{-11} \\ &= 116591802(2)(42)(26) \times 10^{-11}. \end{aligned} \tag{1.39a}$$

This amounts to a difference between experiment and theory of

$$\Delta a_\mu \equiv a_\mu^{(\text{expt})} - a_\mu^{(\text{thy})} = 287(63)(49) \times 10^{-11} \tag{1.39b}$$

² We follow the treatment of Hoecker and Marciano [RPP 12], which lists many references.

or 3.6 times the corresponding one-sigma error. If instead tau decay data are used, the discrepancy between experiment and theory is 2.4σ .

The theoretical values [AoHKN 12] of the magnetic moments a_e and a_μ for both electron and muon are displayed in Table V-1. There is at present no consensus about whether the theoretical predictions are in accord with the experimental determinations, and work continues on this subject. At any rate, these represent an even more stringent test of *QED* than the hyperfine frequency in hydrogen because theory is far less influenced by hadronic effects, and is thus about a factor of 10^4 more precise.

Radiative corrections also modify the form of the Dirac coupling. One effect of this vertex correction is to contribute to the *Lamb shift* which lifts the degeneracy between the $2S_{1/2}$ and $2P_{1/2}$ states of the hydrogen atom. Recall that the fine-structure corrections, computed as perturbations of the atomic hamiltonian, give a total energy contribution

$$\begin{aligned} (\Delta E)_{\text{fine str}} &= (\Delta E)_{\text{Darwin}} + (\Delta E)_{\text{spin-orbit}} + (\Delta E)_{\text{rel kin en}} \\ &= -\frac{7.245 \times 10^{-4} \text{eV}}{n^3} \left(\frac{1}{j + 1/2} - \frac{3}{4n} \right), \end{aligned} \quad (1.40)$$

which depends only upon the quantum numbers n and j . Thus, the $2S_{1/2}$ and $2P_{1/2}$ atomic levels are degenerate to this order, and in fact to all orders. However, the vertex radiative correction breaks the degeneracy, lowering the $2P_{1/2}$ level with respect to the $2S_{1/2}$ level by 1010 MHz. When the anomalous magnetic moment coupling (+68 MHz), the Uehling vacuum polarization potential (-27 MHz), and effects of higher order in α/π are added to this, the result agrees with the experimental value (cf. Table V-1). Since the entire Lamb shift arises from field-theoretic radiative corrections, one must regard the agreement with experiment as strong confirmation for the validity of *QED* and of the renormalization prescription.

The infrared problem

Viewed collectively, the results of this section point to a remarkable success for *QED*. Yet there remains an apparent blemish – the theory still contains an infinity. When the photon ‘mass’ λ is set equal to zero, the vertex modification of Eq. (1.29) diverges logarithmically due to the presence of terms logarithmic in λ^2 . The resolution of this difficulty lies in realizing that any electromagnetic scattering process is unavoidably accompanied by a background of events containing one or more *soft* photons whose energy is too small to be detected. For example, consider Coulomb scattering of electrons from a heavy point source of charge Ze . The spin-averaged cross section for the scattering of unpolarized electrons in the absence of electromagnetic corrections is

$$\frac{d\sigma^{(0)}}{d\Omega} = \frac{Z^2\alpha^2}{4} \cdot \frac{1 - \beta^2 \sin^2 \frac{\theta}{2}}{|\mathbf{p}_e|^2 \beta^2 \sin^4 \frac{\theta}{2}}, \tag{1.41}$$

where $\beta = |\mathbf{p}_e|/E$ is the electron speed. Radiative corrections modify this result. Using the on-shell subtraction prescription and neglecting the anomalous magnetic-moment contribution, one has in the limit $m_e^2 \gg q^2$,

$$\frac{d\sigma}{d\Omega} = \frac{d\sigma^{(0)}}{d\Omega} \left[1 + \frac{2\alpha}{3\pi} \frac{q^2}{m_e^2} \left(\ln \left(\frac{m_e}{\lambda} \right) - \frac{3}{8} \right) + \dots \right] \tag{1.42}$$

from the *QED* vertex correction. This diverges if we attempt to take $\lambda \rightarrow 0$.

However, we must also consider the bremsstrahlung process, in which the scattering amplitude is accompanied by emission of a soft photon of infinitesimal mass λ and four-momentum k^μ . For k_0 sufficiently small, the inelastic bremsstrahlung process cannot be experimentally distinguished from the radiatively corrected elastic scattering of Eq. (1.42). To lowest order in the photon momentum k the invariant amplitude \mathcal{M}_B for bremsstrahlung is³

$$\begin{aligned} \mathcal{M}_B &= \frac{Ze}{\mathbf{q}^2} \bar{u}(p'_e) \left[(-ie\not{\epsilon}) \frac{i}{\not{p}'_e + \not{k} - m_e} (-ie\gamma_0) \right] u(p_e) \\ &\quad + \bar{u}(p'_e) \left[(-ie\gamma_0) \frac{i}{\not{p}_e - \not{k} - m_e} (-ie\not{\epsilon}) \right] u(p_e) \\ &= \mathcal{M}^{(0)} \times e \left(\frac{p'_e \cdot \epsilon}{p'_e \cdot k} - \frac{p_e \cdot \epsilon}{p_e \cdot k} \right), \end{aligned} \tag{1.43}$$

and has the corresponding cross section

$$d\sigma_\gamma = d\sigma^{(0)} e^2 \int' \frac{d^3k}{(2\pi)^3} \frac{1}{2k_0} \sum_{\text{pol}} \left(\frac{p'_e \cdot \epsilon}{p'_e \cdot k} - \frac{p_e \cdot \epsilon}{p_e \cdot k} \right)^2. \tag{1.44}$$

The prime on the integral sign denotes limiting the range of photon energy, $\lambda \leq k_0 \leq \Delta E$, where ΔE is the detector energy resolution. The polarization sum in Eq. (1.44) is performed with the aid of the completeness relation for massive spin-one photons

$$\sum_{\text{pol}} \epsilon_\mu(k) \epsilon_\nu(k) = -g_{\mu\nu} + \frac{k_\mu k_\nu}{\lambda^2}, \tag{1.45}$$

to yield

$$\frac{d\sigma_\gamma}{d\Omega} = \frac{d\sigma^{(0)}}{d\Omega} e^2 \int' \frac{d^3k}{(2\pi)^3} \frac{1}{2k_0} \left(\frac{2p_e \cdot p'_e}{p'_e \cdot k p_e \cdot k} - \frac{m_e^2}{(p_e \cdot k)^2} - \frac{m_e^2}{(p'_e \cdot k)^2} \right). \tag{1.46}$$

³ For simplicity, we shall take the photon as massless in this amplitude, and at the end indicate the effect of this omission.

Performing the angular integration in Eq. (1.46) with the aid of

$$\begin{aligned} \int d\Omega \frac{m_e^2}{(p \cdot k)^2} &= \frac{4\pi}{k_0^2} + \mathcal{O}(\lambda^2), \\ \int d\Omega \frac{2p_e \cdot p'_e}{p'_e \cdot k p_e \cdot k} &= \int_0^1 dx \int d\Omega \frac{2p_e \cdot p'_e}{(k \cdot p_x)^2} + \mathcal{O}(\lambda^2) \\ &= \frac{4\pi}{k_0^2} \left(2 - \frac{q^2}{m_e^2}\right) \int_0^1 dx \left(1 - \frac{q^2}{m_e^2} x(1-x)\right)^{-1} + \mathcal{O}(\lambda^2), \end{aligned} \quad (1.47)$$

we find

$$\frac{d\sigma_\gamma}{d\Omega} = -\frac{d\sigma^{(0)}}{d\Omega} \left[\frac{2\alpha}{3\pi} \frac{q^2}{m_e^2} \left(\ln \left(\frac{2(\Delta E)}{\lambda} \right) - 1 \right) + \mathcal{O} \left(\frac{q^4}{m_e^4} \right) \right]. \quad (1.48)$$

Adding this to the nonradiative cross section of Eq. (1.42), we obtain the finite result,

$$\frac{d\sigma}{d\Omega} + \frac{d\sigma_\gamma}{d\Omega} = \frac{d\sigma^{(0)}}{d\Omega} \left[1 + \frac{2\alpha}{3\pi} \frac{q^2}{m_e^2} \left(\ln \left(\frac{m_e}{2(\Delta E)} \right) + \frac{5}{8} \right) \right]. \quad (1.49)$$

Thus, the net effect of soft-photon emission is to replace the photon mass λ by the detector resolution $2\Delta E$, leaving a finite result.⁴

V-2 The muon

The analysis just presented for the electron can just as well be repeated for the muon. However, the muon has the additional property of being an unstable particle, and in the following we shall focus entirely on this aspect. The subject of muon decay is important because it provides a direct test of the spin structure of the charged weak current. It is also important to be familiar with the calculation of photonic corrections to muon decay, as they are part of the process whereby the Fermi constant G_μ is determined from experiment.

Muon decay at tree level

Muon decay does not proceed like the $2p \rightarrow 1s + \gamma$ transition in atomic hydrogen because the radiative process $\mu \rightarrow e + \gamma$ would conserve neither muon nor electron number and is predicted to be highly suppressed in the Standard Model. Indeed the current bound [Ad *et al.* (MEG collab.) 13] for this mode is extremely tiny, $\mathcal{B}r_{\mu \rightarrow e + \gamma} < 5.7 \times 10^{-13}$ at 90% confidence level.⁵

⁴ As anticipated, the result quoted in Eq. (1.49) is not quite correct, since although we have given the photon an effective mass λ we have not consistently included it, as in Eq. (1.43). In a more careful evaluation the constant $\frac{5}{8}$ is replaced by the value $\frac{11}{24}$.

⁵ See Problem V-1 for a further discussion of $\mu \rightarrow e + \gamma$.

In fact, it is the weak transition $\mu(\mathbf{p}_1, \mathbf{s}) \rightarrow \nu_\mu(\mathbf{p}_2) + e(\mathbf{p}_3) + \bar{\nu}_e(\mathbf{p}_4)$ which is the dominant decay mode of the muon. In the Standard Model, this process occurs through W -boson exchange between the leptons. However, since the momentum transfer is small compared to the W -boson mass, it is possible to express muon decay in terms of the local *Fermi* interaction,

$$\mathcal{L}_{\text{Fermi}} = -\frac{G_\mu}{\sqrt{2}} \bar{\psi}^{(\nu_\mu)} \gamma^\alpha (1 + \gamma_5) \psi^{(\mu)} \bar{\psi}^{(e)} \gamma_\alpha (1 + \gamma_5) \psi^{(\nu_e)} \tag{2.1}$$

$$= -\frac{G_\mu}{\sqrt{2}} \bar{\psi}_{(e)} \gamma^\alpha (1 + \gamma_5) \psi_{(\mu)} \bar{\psi}_{(\nu_\mu)} \gamma_\alpha (1 + \gamma_5) \psi_{(\nu_e)}, \tag{2.2}$$

where the coupling constant G_μ is to be considered a phenomenological quantity determined from the muon lifetime. At tree level, G_μ is related to basic Standard Model parameters as in Eq. (II–3.43). The orderings in Eqs. (2.1)–(2.2) are called, respectively, the *charge-exchange* and *charge-retention* forms of the interaction, and are related by the Fierz transformation of Eq. (C–2.11).

Let us consider the decay of a polarized muon, with rest-frame spin vector $\hat{\mathbf{s}}$, into final states in which spin is not detected. For simplicity, we set the electron mass to zero. The muon decay width is given in terms of a three-body phase space integral by

$$\Gamma_{\mu \rightarrow e \nu_\mu \bar{\nu}_e} = \frac{1}{(2\pi)^5} \frac{1}{2E_1} \int \prod_{j=2}^4 \frac{d^3 p_j}{2E_j} \delta^{(4)}(p_1 - p_2 - p_3 - p_4) \sum_{s_2, s_3, s_4} |\mathcal{M}|^2, \tag{2.3}$$

where in charge-exchange form,

$$\mathcal{M} = \frac{G_\mu}{\sqrt{2}} \bar{u}(\mathbf{p}_2, s_2) \gamma^\alpha (1 + \gamma_5) u(\mathbf{p}_1, s_1) \bar{u}(\mathbf{p}_3, s_3) \gamma_\alpha (1 + \gamma_5) v(\mathbf{p}_4, s_4). \tag{2.4}$$

The muon polarization is described by a four-vector s^μ , which equals $(0, \hat{\mathbf{s}})$ in the muon rest frame. In computing the squared matrix element, we employ

$$u_\beta(\mathbf{p}_1, s_1) \bar{u}_\alpha(\mathbf{p}_1, s_1) = \frac{1}{2} [(m_\mu + \not{p}_1)(1 - \gamma_5 \not{s})]_{\beta\alpha} \tag{2.5}$$

to obtain

$$\sum_{s_2, s_3, s_4} |\mathcal{M}|^2 = 64 G_\mu^2 (p_1 \cdot p_4 p_2 \cdot p_3 - m_\mu p_4 \cdot s p_2 \cdot p_3). \tag{2.6}$$

The neutrino phase space integral is easily found to be

$$\int \frac{d^3 p_2}{2E_2} \frac{d^3 p_4}{2E_4} \delta^{(4)}(Q - p_2 - p_4) p_2^\alpha p_4^\beta = \frac{\pi}{24} (g^{\alpha\beta} Q^2 + 2Q^\alpha Q^\beta), \tag{2.7}$$

where $Q = p_1 - p_3$. For the electron phase space, it is convenient to define a reduced electron energy $x = E_e/W$, where $W = m_\mu/2$ is the maximum electron

energy in the limit of zero electron mass. The standard notation for the electron spectrum involves the so-called *Michel parameters* ρ, δ, ξ whose values depend on the tensorial nature of the beta decay interaction,

$$d^2\Gamma_{\mu \rightarrow e\nu_\mu\bar{\nu}_e} = \frac{G_\mu^2 m_\mu^5}{192\pi^3} \left[6(1-x) + 4\rho \left(\frac{4x}{3} - 1 \right) - 2\xi \cos\theta \left(1 - x + 2\delta \left(\frac{4x}{3} - 1 \right) \right) \right] x^2 dx \sin\theta d\theta. \quad (2.8)$$

For the $V - A$ chiral structure of the Fermi model, we predict

$$\rho = \delta = 0.75, \quad \xi = 1.0, \quad (2.9a)$$

in good agreement with the current experimental values [RPP 12],

$$\rho = 0.74979 \pm 0.00026, \quad \delta = 0.75047 \pm 0.00034, \quad \xi P_\mu \delta / \rho = 1.0018^{+0.0016}_{-0.0007} \quad (2.9b)$$

where P_μ is the longitudinal muon polarization from pion decay ($P_\mu = P_\nu / E_\nu = 1$ in $V - A$ theory). In making comparisons between Eq. (2.9a) and Eq. (2.9b), one should first subtract from the data corrections due to radiative effects. Upon integration over the electron phase space, Eq. (2.8) gives rise to the well-known formula,

$$\Gamma_{\mu \rightarrow e\nu_\mu\bar{\nu}_e} = \frac{1}{\tau_{\mu \rightarrow e\nu_\mu\bar{\nu}_e}} = \frac{G_\mu^2 m_\mu^5}{192\pi^3}. \quad (2.10)$$

This relation has been used to provide an order-of-magnitude estimate for decay rates of heavy leptons and quarks.

Precise determination of G_μ

Thus far, we have worked to lowest order in the local Fermi interaction and have assumed massless final state particles. This is not sufficient to describe results from modern experiments, e.g., the recent measurement of $\tau_{\mu \rightarrow e\nu_\mu\bar{\nu}_e}$ by Webber *et al.* [We *et al.* (MuLan collab.) 11] is 15 times as precise as any previous determination and provides a value of G_μ with an uncertainty of only 0.6 ppm.

Including corrections to Eq. (2.10) yields

$$\Gamma_{\mu \rightarrow e\nu_\mu\bar{\nu}_e} = \frac{G_\mu^2 m_\mu^5}{192\pi^3} f(x) r_\gamma(\hat{\alpha}(m_\mu), x) r_W(y_\mu), \quad (2.11a)$$

where $f(x)$ is a phase space factor, with $x \equiv m_e^2 / m_\mu^2$,

$$f(x) = 1 - 8x + 8x^3 - x^4 - 12x^2 \ln x \simeq 0.999812961, \quad (2.11b)$$

Table V–2. *Determinations of Fermi-model couplings.*

Factor	Determination
G_μ	Muon decay
$G_\tau^{(\ell)}$	Tau decay into lepton ℓ
G_β	G_μ plus <i>QED</i> theory
$G_\beta V_{ud}$	{ Nuclear beta decay $\pi\ell_3$
$G_\beta V_{us}$	{ Hyperon beta decay $K\ell_3$
$G_\beta V_{ud} F_\pi$	Pion beta decay ($\pi\ell_2$)
$G_\beta V_{us} F_K$	Kaon beta decay ($K\ell_2$)

and $r_W(y_\mu) = 1 + 3y_\mu/5 + \dots$ is a W -boson propagator correction, with $y_\mu \equiv m_\mu^2/M_W^2$.⁶ The quantity $r_\gamma(\hat{\alpha}(m_\mu), x)$ provides a perturbative expression of the photonic radiative corrections,

$$r_\gamma(\hat{\alpha}, x) = H_1(x) \frac{\hat{\alpha}(m_\mu)}{\pi} + H_2(x) \frac{\hat{\alpha}^2(m_\mu)}{\pi^2} + \dots, \quad (2.11c)$$

where $\hat{\alpha}(m_\mu)$ refers to the $\overline{\text{MS}}$ subtracted quantity

$$\hat{\alpha}(m_\mu)^{-1} = \alpha^{-1} + \frac{1}{3\pi} \ln x + \dots \simeq 135.901. \quad (2.11d)$$

The functions $H_1(x)$, $H_2(x)$ appear, together with references to original work, in Chap. 10 of [RPP 12]. In the subsection to follow, we will calculate the leading-order contribution to r_γ . The above theoretical relations lead to the determination

$$G_\mu = 1.1663787(6) \times 10^{-5} \text{ GeV}^{-2}. \quad (2.12)$$

The above analysis serves to define the Fermi constant in the context of muon decay. Fermi couplings $G_\tau^{(\ell)}$ for the weak leptonic transitions $\tau^- \rightarrow e^- + \bar{\nu}_e + \nu_\tau$ and $\tau^- \rightarrow \mu^- + \bar{\nu}_\mu + \nu_\tau$ can likewise be defined and compared with G_μ (see Sect. V–3). However, for weak semileptonic transitions of hadrons (e.g. nuclear beta decay) the photonic corrections are *not* identical to those in muon decay because quark charges differ from lepton charges. Such processes define instead a quantity called G_β , and we shall present in Sect. VII–1 a calculation of G_β for the case of pion decay (cf. Eq. (VII–1.31)). As seen in Table V–2, determinations involving G_β generally contain quark mixing factors and also meson decay

⁶ It is possible to study muon decay corrections either within just the Fermi effective theory or with the full Standard Model. For the former choice $r_W(y_\mu)$ is omitted in Eq. (2.11a), whereas for the latter it is included. Which choice is made affects details of higher-order corrections. We have opted to follow the first edition of this book by including $r_W(y_\mu)$. In fact, its effect is numerically tiny, affecting only the final decimal place in the value of G_μ given in Eq. (2.12).

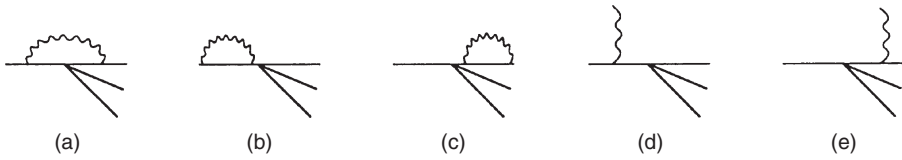


Fig. V-1 Contributions to muon decay from (a) vertex, (b)–(c) wavefunction renormalization, and (d)–(e) bremsstrahlung amplitudes.

constants. Marciano [Ma 11] has used, among other processes, semileptonic decays (nuclear, kaon and *B*-meson) and CKM unitarity to determine the Fermi constant without recourse to muon decay. He finds $G_F^{(CKM)} = 1.166309(350) \times 10^{-5} \text{ GeV}^2$, which is the second most accurate determination after the muon decay value of Eq. (2.12), but relatively far less accurate.

Leading-order photonic correction

Computation of the lowest order electron and *W*-boson mass corrections appearing in Eq. (2.10) is not difficult, and is left to Prob. V-2. However, the *QED* radiative correction is rather more formidable, and it is to that which we now turn our attention. Rather than attempt a detailed presentation, we summarize the analysis of [GuPR 80]. We shall work in Feynman gauge, and employ the charge-retention ordering for the Fermi interaction. There is an advantage to performing the calculation as if the muon existed in a spacetime of arbitrary dimension *d*. Working in *d* = 4 dimensions entails factors which are logarithmic in the electron mass and which would forbid the simplifying assumption $m_e = 0$. Dimensional regularization frees one from this restriction, and such potential singularities become displayed as poles in the variable $\epsilon = (4 - d)/2$. Although there would appear to be difficulty in extending the Dirac matrix γ_5 to arbitrary spacetime dimensions, this turns out not to be a problem here. The set of radiative corrections consists of three parts, which are displayed in Fig. V-1, (i) vertex (Fig. V-1(a)), (ii) self-energy (Fig. V-1(b)–(c)), and (iii) bremsstrahlung (Fig. V-1(d)–(e)). We shall begin with the bremsstrahlung part of the calculation and then proceed to the vertex and self-energy contributions.

The amplitude for the bremsstrahlung (*B*) process $\mu(\mathbf{p}_1) \rightarrow \nu_\mu(\mathbf{p}_2) + e(\mathbf{p}_3) + \bar{\nu}_e(\mathbf{p}_4) + \gamma(\mathbf{p}_5)$ is given by

$$\mathcal{M}_B = \frac{eG_\mu}{\sqrt{2}} \bar{u}(\mathbf{p}_2) \gamma^\alpha (1 + \gamma_5) v(\mathbf{p}_4) \times \bar{u}(\mathbf{p}_3) \left[\gamma_\alpha (1 + \gamma_5) \frac{1}{\not{p}_1 - \not{p}_5 - m_\mu} \not{\epsilon} + \not{\epsilon} \frac{1}{\not{p}_3 + \not{p}_5 - m_e} \gamma_\alpha (1 + \gamma_5) \right] u(\mathbf{p}_1), \tag{2.13}$$

where ϵ is the photon polarization vector. The spin-averaged bremsstrahlung transition rate for d spacetime dimensions in the muon rest frame is then given by⁷

$$\Gamma_B = \frac{1}{2m_\mu} \int \prod_{j=2}^5 \left(\frac{d^{d-1} p_j}{2E_j (2\pi)^{d-1}} \right) (2\pi)^d \delta^{(d)}(Q' - p_2 - p_4) \frac{1}{2} \sum_{\text{spins}} |\mathcal{M}_B|^2, \tag{2.14}$$

where $Q' \equiv Q - p_5 = p_1 - p_3 - p_5$. A lengthy analysis yields a result which can be expanded in powers of $\epsilon = (4 - d)/2$ to read

$$\Gamma_B = \frac{G_\mu^2 m_\mu^5}{192\pi^3} \frac{3\alpha}{4} \left(\frac{m_\mu^3}{32\pi^{3/2}} \right)^{-2\epsilon} \frac{\Gamma(2 - \epsilon)}{\Gamma(\frac{3}{2} - \epsilon) \Gamma(\frac{5}{2} - \epsilon) \Gamma(5 - 3\epsilon)} \times \left(\frac{6}{\epsilon^2} - \frac{5 - 6\gamma}{\epsilon} - 5\gamma + 3\gamma^2 - \frac{7\pi^2}{2} + \frac{215}{6} + \mathcal{O}(\epsilon) \right). \tag{2.15}$$

Observe that singularities are encountered as $\epsilon \rightarrow 0$.

The radiative correction (R) contribution to the muon transition rate is given by

$$\Gamma_R = \frac{1}{2m_\mu} \int \prod_{j=2}^4 \left(\frac{d^{d-1} p_j}{2E_j (2\pi)^{d-1}} \right) (2\pi)^d \delta^{(d)}(Q - p_2 - p_4) \frac{1}{2} \sum_{\text{spins}} |\mathcal{M}|_{\text{int}}^2, \tag{2.16}$$

where $|\mathcal{M}|_{\text{int}}^2$ is the interference term between the Fermi-model amplitudes, which are, respectively, zeroth order ($\mathcal{M}^{(0)}$) and first order ($\mathcal{M}^{(1)}$) in e^2 ,

$$|\mathcal{M}|_{\text{int}}^2 = \mathcal{M}^{(0)*} \mathcal{M}^{(1)} + \mathcal{M}^{(1)*} \mathcal{M}^{(0)}. \tag{2.17}$$

The first-order amplitude can be written as a product of neutrino factors and a term (\mathcal{M}_R) containing radiative corrections of the charged leptons,

$$\mathcal{M}^{(1)} = \frac{e^2 G_\mu}{\sqrt{2}} \bar{u}(\mathbf{p}_2) \gamma_\alpha (1 + \gamma_5) v(\mathbf{p}_4) \mathcal{M}_R^\alpha. \tag{2.18}$$

The quantity \mathcal{M}_R^α is itself expressible as the sum of vertex (V) and self-energy (SE) contributions,

$$\mathcal{M}_R^\alpha = \bar{u}(\mathbf{p}_3) (\mathcal{M}_V^\alpha + \mathcal{M}_{SE}^\alpha) u(\mathbf{p}_1). \tag{2.19}$$

The vertex modification of Fig. V-1(c)

$$\mathcal{M}_V^\alpha = \frac{1}{i} \int \frac{d^4 k}{(2\pi)^4} \frac{\gamma^\mu (\not{p}_3 - \not{k}) \gamma^\alpha (1 + \gamma_5) (\not{p}_1 - \not{k} + m_\mu) \gamma_\mu}{k^2 (p_3 - k)^2 [(p_1 - k)^2 - m_\mu^2]}, \tag{2.20}$$

⁷ Since the result that we seek is finite and scale independent, in this section we shall suppress the scale parameter μ introduced in Eq. (II-1.21b).

has the same form as the electromagnetic vertex correction for the electron discussed previously (cf. Eq. (1.19)) except that it contains the weak vertex $\gamma^\alpha(1+\gamma_5)$. Upon employing the Feynman parameterization in Eq. (2.20) and using the muon equation of motion, the extension of the vertex amplitude to d dimensions can ultimately be expressed in terms of hypergeometric functions,

$$\mathcal{M}_V^\alpha = 4\Gamma\left(3 - \frac{d}{2}\right) \frac{m_\mu^{-(4-d)}}{(4\pi)^{d/2}} \left[\gamma^\alpha (1 + \gamma_5) A_1 + (1 - \gamma_5) \frac{p_1^\alpha B + p_3^\alpha C}{m_\mu} \right], \tag{2.21}$$

where

$$\begin{aligned} A_1 &= \frac{F\left(3 - \frac{d}{2}, 1; \frac{d}{2}; \xi\right)}{(d-3)(d-2)} - \frac{(d-3)F\left(2 - \frac{d}{2}, 1; \frac{d}{2}; \xi\right)}{(d-4)(d-2)} \\ &\quad - \frac{(1-\xi)F\left(3 - \frac{d}{2}, 1; \frac{d}{2} - 1, \xi\right)}{(d-4)^2(d-3)}, \tag{2.22} \\ B &= \frac{F\left(3 - \frac{d}{2}, 1; \frac{d}{2} + 1; \xi\right)}{d}, \\ C &= \frac{2F\left(3 - \frac{d}{2}, 2; \frac{d}{2} + 1; \xi\right)}{d(d-2)} - \frac{2F\left(3 - \frac{d}{2}, 1; \frac{d}{2}; \xi\right)}{(d-2)(d-3)}. \end{aligned}$$

For the muon self-energy amplitude of Fig. (V-1(d)), we write

$$\Sigma(p) = -i \int \frac{d^d q}{(2\pi)^d} \frac{\gamma^\lambda (\not{p} - \not{q} + m_\mu) \gamma_\lambda}{q^2 (q^2 - 2p \cdot q + p^2 - m_\mu^2)}, \tag{2.23}$$

remembering that a factor of e^2 has already been extracted in Eq. (2.18). Implementing the Feynman parameterization and integrating over the virtual momentum yields an expression,

$$\Sigma(p) = \frac{\Gamma\left(2 - \frac{d}{2}\right)}{(4\pi)^{d/2}} \frac{1}{m_\mu^{4-d}} \int_0^1 dx [m_\mu d + x(2-d)\not{p}] \frac{(1-x)^{(4-d)/2}}{\left(1-x\frac{p^2}{m^2}\right)^{(4-d)/2}}, \tag{2.24}$$

which with the aid of Eq. (C-5.5) in App. C can be written in terms of hypergeometric functions,

$$\begin{aligned} \Sigma(p) &= \frac{\Gamma\left(2 - \frac{d}{2}\right)}{(4\pi)^{d/2}} \frac{1}{m_\mu^{4-d}} \left[m_\mu \frac{2d}{d-2} F\left(\frac{4-d}{2}, 1; \frac{d}{2}; \frac{p^2}{m_\mu^2}\right) \right. \\ &\quad \left. - \not{p} \frac{4}{d} F\left(\frac{4-d}{2}, 2; \frac{d+2}{2}; \frac{p^2}{m_\mu^2}\right) \right]. \tag{2.25} \end{aligned}$$

When the self-energy is expanded in powers of $\not{p} - m_\mu$, the leading term is just the mass shift, which is removed by mass renormalization. We require the \not{p} -derivative

of $\Sigma(p)$ evaluated at $\not{p} = m_\mu$. Being careful while carrying out the differentiation to interpret p^2 factors as $\not{p}\not{p}$, we find

$$\left. \frac{\partial \Sigma}{\partial \not{p}} \right|_{\not{p}=m_\mu} = \frac{\Gamma(2 - \frac{d}{2})}{(4\pi)^{d/2}} \frac{1}{m_\mu^{4-d}} \frac{1-d}{d-3}. \quad (2.26)$$

It is this quantity multiplied by the vertex $\gamma^\alpha(1 + \gamma_5)$ which ultimately gives rise to \mathcal{M}_{SE}^α . However, in addition to mass renormalization there is also wavefunction renormalization, whose effect is to reduce the above quantity by a factor of 2, yielding

$$\mathcal{M}_{SE}^\alpha = \frac{\Gamma(3 - \frac{d}{2})}{(4\pi)^{d/2}} \frac{1}{m_\mu^{4-d}} \frac{1-d}{4(4-d)(d-3)} \gamma^\alpha(1 + \gamma_5). \quad (2.27)$$

In principle, there also exists the electron self-energy contribution. As can be verified by direct calculation, this vanishes because the electron is taken as massless. Thus, we conclude that

$$\begin{aligned} \mathcal{M}_{SE}^\alpha &= 4\Gamma\left(3 - \frac{d}{2}\right) \frac{m_\mu^{d-4}}{(4\pi)^{d/2}} A_2 \gamma^\alpha(1 + \gamma_5), \\ A_2 &= -\frac{1}{4} \frac{d-1}{(4-d)(d-3)}. \end{aligned} \quad (2.28)$$

The net effect of the self-energy contribution is to replace A_1 in the vertex amplitude of Eq. (2.21) by $A = A_1 + A_2$.

Insertion of the radiatively corrected amplitudes into Eq. (2.16) leads to a transition rate Γ_R , which expanded to lowest order in $\epsilon = (4-d)/2$, has the form

$$\begin{aligned} \Gamma_R &= \frac{G_\mu^2 m_\mu^5}{192\pi^3} \frac{3\alpha}{4} \left(\frac{m_\mu^3}{32\pi^{3/2}} \right)^{-2\epsilon} \frac{\Gamma(2-\epsilon)}{\Gamma(\frac{3}{2}-\epsilon) \Gamma(\frac{5}{2}-\epsilon) \Gamma(5-3\epsilon)} \\ &\times \left(-\frac{6}{\epsilon^2} + \frac{5-6\gamma}{\epsilon} + 5\gamma - 3\gamma^2 - \frac{5\pi^2}{2} + \frac{5}{3} + \mathcal{O}(\epsilon) \right). \end{aligned} \quad (2.29)$$

Like the bremsstrahlung contribution, the radiatively corrected decay rate is found to be singular in the $\epsilon \rightarrow 0$ limit. However, the final result which is obtained by adding the radiative correction of Eq. (2.29) to that of the bremsstrahlung expression of Eq. (2.15) is found to be free of divergences,

$$\delta\Gamma_{\text{muon}}^{(\text{QED})} = \Gamma_R + \Gamma_B = -\frac{G_\mu^2 m_\mu^5}{192\pi^3} \frac{\alpha(m_\mu)}{2\pi} \left(\pi^2 - \frac{25}{4} \right), \quad (2.30)$$

which is the leading-order contribution to the function r_γ of Eq. (2.11c).

V-3 The τ lepton

The heaviest known lepton is τ (1777), having been discovered in e^+e^- collisions in 1975. There exists also an associated neutrino ν_τ with current mass limit $m_{\nu_\tau} < 18.2$ MeV. Like the muon, the τ can decay via purely *leptonic* modes,

$$\tau^- \rightarrow \begin{cases} \mu^- + \bar{\nu}_\mu + \nu_\tau \\ e^- + \bar{\nu}_e + \nu_\tau \\ \vdots \end{cases} \quad (3.1)$$

However, a new element exists in τ decay, for numerous *semileptonic* modes are also present,

$$\tau^- \rightarrow \begin{cases} \pi^- + \nu_\tau \\ \pi^- + \pi^0 + \nu_\tau \\ \vdots \end{cases} \quad (3.2)$$

Experiment has revealed the semileptonic sector to be an important component of tau decay, e.g., [Am *et al.* (Heavy Flavor Averaging Group collab.) 12],

$$R_\tau \equiv \frac{\Gamma_{\text{semileptonic}}}{\Gamma_{\tau \rightarrow e\bar{\nu}_e\nu_\tau}} \Big|_{\text{expt}} = \frac{1 - \text{Br}_{\tau \rightarrow e\bar{\nu}_e\nu_\tau} - \text{Br}_{\tau \rightarrow \mu\bar{\nu}_\mu\nu_\tau}}{\text{Br}_{\tau \rightarrow e\bar{\nu}_e\nu_\tau}} = 3.6280 \pm 0.0094, \quad (3.3)$$

where Br denotes branching ratio. It is possible to obtain a simple but naive estimate of R_τ as follows. Because the τ is lighter than any charmed hadron, semileptonic decay amplitudes must involve the quark charged weak current

$$J_{\text{ch}}^\mu = V_{\text{ud}} \bar{d}\gamma^\mu(1 + \gamma_5)u + V_{\text{us}} \bar{s}\gamma^\mu(1 + \gamma_5)u, \quad (3.4)$$

where V_{ud} and V_{us} are CKM mixing elements. Neglect of all final state masses and of effects associated with quark hadronization (an assumption only approximately valid at this relatively low energy) implies the estimates

$$\begin{aligned} R_\tau^{(\text{naive})} &\simeq N_c [|V_{\text{ud}}|^2 + |V_{\text{us}}|^2] \simeq N_c \xrightarrow{N_c=3} 3.0, \\ \text{Br}_{\tau \rightarrow e\bar{\nu}_e\nu_\tau}^{(\text{naive})} &\simeq \text{Br}_{\tau \rightarrow \mu\bar{\nu}_\mu\nu_\tau}^{(\text{naive})} \simeq \frac{1}{2 + N_c} \xrightarrow{N_c=3} 0.2, \end{aligned} \quad (3.5)$$

where N_c is the number of quark color degrees of freedom. The above analysis although rough, nonetheless yields estimates for R_τ , $\tau \rightarrow e\bar{\nu}_e\nu_\tau$ and $\tau \rightarrow \mu\bar{\nu}_\mu\nu_\tau$ in approximate accord with the corresponding experimental values. Also, it is not inconsistent with our belief that $N_c = 3$. However, we can and will improve upon this state of affairs (cf. Eq. (3.27b)) and as a bonus will obtain a determination of the strong coupling $\alpha_s(m_\tau)$.

Exclusive leptonic decays

The momentum spectra of the electron and muon modes also probe the nature of τ decay. The Michel parameter ρ of Eq. (2.8) should equal 0.75 for the usual $V - A$ currents, zero for the combination $V + A$ and 0.375 for V or A separately. The observed value $\rho = 0.745 \pm 0.008$ is in accord with the $V - A$ structure.

The τ leptonic decays afford an opportunity to test the principle of *lepton universality*, i.e., the premise that the only physical difference among the charged leptons is that of mass. In particular, all the charged leptons are expected to have identical charged current weak couplings, cf. Eqs. (II-3.36),(II-3.37),

$$g_{2e} = g_{2\mu} = g_{2\tau} \equiv g_2 \quad (\text{universality condition}). \tag{3.6}$$

This has been tested in [Am *et al.* (Heavy Flavor Averaging Group collab.) 12], using the following Standard Model description for the leptonic decay mode of a heavy lepton L ,

$$\Gamma_{L \rightarrow \nu_L \ell \bar{\nu}_\ell} = \frac{G_L G_\ell m_L^5}{192\pi^3} f(x)r_\gamma(m_L)r_W(y_L),$$

$$G_\ell = \frac{g_{2\ell}^2}{4\sqrt{2}M_W^2}, \quad r_\gamma(m_L) = 1 + \frac{\alpha(m_L)}{2\pi} \left(\frac{25}{4} - \pi^2 \right), \tag{3.7}$$

where $f(x)$ is as in Eq. (2.11b) and $r_W(y_L) = 1 + 3m_L^2/(5M_W^2 + \dots)$. They find [Am *et al.* (Heavy Flavor Averaging Group collab.) 12],

$$\frac{g_{2\tau}}{g_{2\mu}} = 1.0006 \pm 0.0021, \quad \frac{g_{2\tau}}{g_{2e}} = 1.0024 \pm 0.0021, \quad \frac{g_{2\mu}}{g_{2e}} = 1.0018 \pm 0.0014, \tag{3.8}$$

consistent with the universality condition of Eq. (3.6).

There are other ways to study the universality principle. Looking forward to Chap. XVI, we shall exhibit in Eq. (XVI-2.6) the result of testing lepton universality with the decays $Z^0 \rightarrow \ell\bar{\ell}$ ($\ell = e, \mu, \tau$). Unlike the above example in Eq. (3.8), the Z^0 decay widths are functions of *neutral* weak coupling constants. Yet another approach, which uses charged current couplings, is to compare leptonic and semileptonic decays, like $H \rightarrow \mu\bar{\nu}_\mu$ (where H can be a pion, kaon, etc.) with $\tau \rightarrow H\nu_\tau$.

Exclusive semileptonic decays

Matters are somewhat more complex for the hadronic final states, due in part to the large number of modes. Still, for many of these we can make detailed confrontation of theoretical predictions with experimental results. We begin by noting that the

semileptonic decay amplitude factorizes into purely leptonic and hadronic matrix elements of the weak current,

$$\begin{aligned} \mathcal{M}_{\text{semilept}} &= \frac{G_\mu}{\sqrt{2}} L^\mu H_\mu, \\ L^\mu &= \langle \nu_\tau(\mathbf{p}') | J_{\text{lept}}^\mu | \tau(\mathbf{p}) \rangle = \bar{v}_\tau(\mathbf{p}') \Gamma_L^\mu \tau(\mathbf{p}), \\ H_\mu &= \langle \text{hadron} | (J_\mu^{\text{qk}})^\dagger | 0 \rangle = \langle \text{hadron} | V_{\text{ud}}^* \bar{d} \Gamma_\mu^L u + V_{\text{us}}^* \bar{s} \Gamma_\mu^L u | 0 \rangle, \end{aligned} \quad (3.9)$$

where $\Gamma_\mu^L \equiv \gamma_\mu(1 + \gamma_5)$. In the following, we analyze some modes containing a single meson,

$$\tau^- \rightarrow \text{meson} + \nu_\tau \quad (\text{meson} = \pi^-, K^-, \rho^-(770), K^{*-}(892)). \quad (3.10)$$

Weak-current matrix elements which connect the vacuum with spin-parity $J^P = 0^-, 1^+$ hadrons are sensitive to only the axial-vector current, whereas $J^P = 0^+, 1^-$ states arise from the vector current. In each case, the vacuum-to-meson matrix element has a form dictated up to a constant by Lorentz invariance,

$$\langle \pi^-(\mathbf{q}) | [\bar{d} \gamma_\mu \gamma_5 u] (0) | 0 \rangle \equiv -i\sqrt{2} F_\pi q_\mu, \quad (3.11a)$$

$$\langle K^-(\mathbf{q}) | [\bar{s} \gamma_\mu \gamma_5 u] (0) | 0 \rangle \equiv -i\sqrt{2} F_K q_\mu, \quad (3.11b)$$

$$\langle \rho^-(\mathbf{q}, \lambda) | [\bar{d} \gamma_\mu u] (0) | 0 \rangle \equiv \sqrt{2} g_\rho \epsilon_\mu^*(\mathbf{q}, \lambda), \quad (3.11c)$$

$$\langle K^{*-}(\mathbf{q}, \lambda) | [\bar{s} \gamma_\mu u] (0) | 0 \rangle \equiv \sqrt{2} g_{K^*} \epsilon_\mu^*(\mathbf{q}, \lambda), \quad (3.11d)$$

where the quantities g_ρ and g_{K^*} are the vector meson decay constants. These quantities contribute to the transition rates for pseudoscalar (p) and vector (v) emission, and we find from straightforward calculations

$$\begin{aligned} \Gamma_{\tau \rightarrow p\nu_\tau} &= \eta_{\text{KM}} G_\mu^2 m_\tau^3 \frac{F_p^2}{8\pi} \left(1 - \frac{m_p^2}{m_\tau^2}\right)^2, \\ \Gamma_{\tau \rightarrow v\nu_\tau} &= \eta_{\text{KM}} \frac{G_\mu^2}{8\pi} \left(\frac{g_v}{m_v^2}\right)^2 m_\tau^3 m_v^2 \left(1 - \frac{m_v^2}{m_\tau^2}\right)^2 \left(1 + 2\frac{m_v^2}{m_\tau^2}\right), \end{aligned} \quad (3.12)$$

where m_p, m_v are the meson masses, $\eta = |V_{\text{ud}}|^2$ for $\Delta S = 0$ decay and $\eta = |V_{\text{us}}|^2$ for $\Delta S = 1$ decay.

It is possible to use the above formulae to extract constants such as F_π, \dots, g_{K^*} from tau decay data. However, such quantities are obtained more precisely from other processes and, in practice, one employs them in tau decay to make branching-ratio predictions. Although QCD-lattice studies have steadily improved on their predictions of such constants, we shall focus instead on phenomenological determinations. In Chap. VII, we shall show how the values $F_\pi = 92.21$ MeV and $F_K/F_\pi = 1.197$ are found from a careful analysis of pion and kaon leptonic weak

Table V-3. *Some hadronic modes in tau decay.*

Mode	Hadronic input	Br [thy] ^a	Br [expt] ^a
$\tau^- \rightarrow \pi^- + \nu_\tau$	$c_1 F_\pi$	11.4	10.83 ± 0.06
$\tau^- \rightarrow K^- + \nu_\tau$	$c_3 s_1 F_K$	0.8	0.70 ± 0.01
$\tau^- \rightarrow \rho^- + \nu_\tau$	$c_1 g_\rho$	23.4 ± 0.8	25.52 ± 0.9
$\tau^- \rightarrow K^{*-} + \nu_\tau$	$c_3 s_1 g_{K^*}$	1.1 ± 0.1	1.33 ± 0.13
$\tau^- \rightarrow \pi^- \pi^- \pi^+ \pi^0 \nu_\tau$	$\sigma(e^+ e^- \rightarrow \text{hadr})$	4.9	4.76 ± 0.06
$\tau^- \rightarrow \pi^- \pi^0 \pi^0 \pi^0 \nu_\tau$	$\sigma(e^+ e^- \rightarrow \text{hadr})$	0.98	1.05 ± 0.07

^aBranching ratios are given in percent.

decay. Interestingly, the hadronic matrix elements which contribute there are just the conjugates of those appearing in Eqs. (3.11a), (3.11b). By contrast, the quantity g_ρ is obtained not from weak decay data, but rather from an electromagnetic decay such as $\rho^0 \rightarrow e\bar{e}$. That the *same* quantity g_ρ should occur in both weak and electromagnetic transitions is a consequence of the isospin structure of quark currents. That is, the electromagnetic current operator is expressed in terms of octet vector current operators by $J_\mu^{\text{em}} = V_\mu^3 + \frac{1}{\sqrt{3}} V_\mu^8$. Since the latter component is an isotopic scalar whereas the ρ meson carries isospin one, it follows from the Wigner–Eckart theorem that

$$\langle 0 | J_\mu^{\text{em}} | \rho^0(\mathbf{p}) \rangle = \langle 0 | V_\mu^3 | \rho^0(\mathbf{p}) \rangle = \frac{1}{\sqrt{2}} \langle 0 | V_\mu^{1+i2} | \rho^-(\mathbf{p}) \rangle = g_\rho \epsilon_\mu(\mathbf{p}). \quad (3.13)$$

The transition rate for the electromagnetic decay $\rho^0 \rightarrow e\bar{e}$ is given, with final state masses neglected, by

$$\Gamma_{\rho^0 \rightarrow e\bar{e}} = \frac{4\pi\alpha^2}{3} \left(\frac{g_\rho}{m_\rho^2} \right)^2 m_\rho, \quad (3.14)$$

from which we find $g_\rho/m_\rho^2 = 0.198 \pm 0.009$. The $K^{*-}\nu_\tau$ mode can be estimated by using the flavor- $SU(3)$ relation $g_{K^*} = g_\rho$. The predictions for single-hadron branching ratios are collected in Table V-3, and are seen to be in satisfactory agreement with the observed values.

A somewhat different approach can be used to obtain predictions for strangeness-conserving modes with $J^P = 1^-$. Since matrix elements of the vector-charged current can be obtained through an isospin rotation from the isovector part of the $e\bar{e}$ annihilation cross section into hadrons, we can write for a given neutral $I = 1$ hadronic final state f^0 ,

$$\sigma_{e\bar{e} \rightarrow f^0}^{(I=1)} = \frac{8\pi^2\alpha^2}{q^2} \Pi_f^0(q^2), \quad (3.15)$$

where we have defined

$$\sum_{f^0} (2\pi)^3 \delta^{(4)}(q - p_{f^0}) \langle f^0 | J_\mu^{(3)} | 0 \rangle \langle f^0 | J_\nu^{(3)} | 0 \rangle^* \equiv \Pi_f^0(q^2) (-q^2 g_{\mu\nu} + q_\mu q_\nu). \tag{3.16}$$

The τ^- transition into the isotopically related charged state f^- ,

$$|f^-\rangle \equiv \frac{1}{\sqrt{2}}(I_1 - iI_2)|f^0\rangle, \tag{3.17}$$

is governed by the *same* function $\Pi_f(q^2)$ of hadronic final states as occurs in Eq. (3.15). Including the lepton current and relevant constants, and performing the integration over ν_τ phase space yields a decay rate

$$\Gamma_{\tau \rightarrow f \nu_\tau} = \frac{G_\mu^2 |V_{ud}|^2 S_{EW}}{32\pi^2 m_\tau^3} \int_0^{m_\tau^2} dq^2 (m_\tau^2 - q^2)^2 (m_\tau^2 + 2q^2) \Pi_f^-(q^2), \tag{3.18}$$

where S_{EW} is given in Eq. (3.25c). The content of Eq. (3.18) is often expressed as a ratio,

$$\frac{\Gamma_{\tau \rightarrow f \nu_\tau}}{\Gamma_{\tau \rightarrow e \nu_\tau \bar{\nu}_e}} = \frac{3|V_{ud}|^2 S_{EW}}{2\pi\alpha^2 m_\tau^8} \int_0^{m_\tau^2} ds (m_\tau^2 - s)^2 (m_\tau^2 + 2s) s \sigma_{e^+e^- \rightarrow f^0}^{(I=1)}(s). \tag{3.19}$$

Thus, we find, e.g., for 4π final states, the results listed in Table V-3.

There exist numerous additional hadronic decay modes of the τ lepton. Examples include final hadronic states containing $K\bar{K}$, $K\bar{K}\pi$, etc., and it is possible to analyze each of these with various degrees of theoretical confidence. Another interesting use of the τ semileptonic decay has been to confirm by inference the fundamental structure of the weak quark current from the absence of the mode $\tau^- \rightarrow \pi^- \eta \nu_\tau$. This mode, proceeding through the vector current, would violate G -parity invariance. Here G -parity refers to the product of charge conjugation and a rotation by π radians about the 2-axis in isospin space,

$$G \equiv C e^{-i\pi I_2}. \tag{3.20}$$

A weak current which could induce a $\Delta G \neq 0$ transition is referred to as a *second-class* current. Such currents do not occur naturally within the quark model. The $\pi^- \eta \nu_\tau$ mode has not been detected, with an existing sensitivity [RPP 12] of $\text{Br}_{\tau \rightarrow \pi \eta \nu_\tau} < 9.9 \times 10^{-5}$. This result, consistent with the absence of second-class currents, fits securely within the framework of the Standard Model.

Inclusive semileptonic decays

The inclusive semileptonic decay of the tau is denoted as $\tau \rightarrow \nu_\tau + X$, where X represents the sum over all kinematically allowed hadronic states. Let us restrict

our attention to the Cabibbo-allowed component, i.e., decay into an even or odd number of pions. The decay rate at invariant squared-energy s is

$$\frac{d\Gamma [\tau \rightarrow \nu_\tau (\begin{smallmatrix} \text{even} \\ \text{odd} \end{smallmatrix})]}{ds} = \frac{G_\mu^2 V_{ud}^2}{8\pi m_\tau^3} (m_\tau^2 - s)^2 \left[(m_\tau^2 + 2s) \begin{pmatrix} \rho_V(s) \\ \rho_A(s) \end{pmatrix} + m_\tau^2 \begin{pmatrix} 0 \\ \rho_A^{(0)}(s) \end{pmatrix} \right], \quad (3.21)$$

as expressed in terms of the so-called *vector* and *axial-vector spectral functions*, spin-one $\rho_V(s)$, $\rho_A(s)$ and spin-zero $\rho_A^{(0)}(s)$.

We can gain some physical understanding of the spectral functions by first studying the propagator $i\Delta(x)$ for a free, scalar field $\varphi(x)$ (cf. Eq. (C–2.12)). Its Fourier transform,

$$\Pi(q^2) = \frac{1}{\mu^2 - q^2 - i\epsilon} \quad \text{with} \quad \mathcal{Im}\Pi(q^2) = \pi\delta(q^2 - \mu^2), \quad (3.22)$$

reveals that the free field $\varphi(x)$ excites the vacuum to just the single state with $q^2 = \mu^2$. For the $V - A$ currents which induce the inclusive tau decay, the momentum space propagators are written

$$\begin{aligned} & i \int d^4x e^{iq \cdot x} \langle 0 | T (V_3^\mu(x) V_3^\nu(0) - A_3^\mu(x) A_3^\nu(0)) | 0 \rangle \\ & = (q^\mu q^\nu - q^2 g^{\mu\nu}) \left(\Pi_{V,3}^{(1)}(q^2) - \Pi_{A,3}^{(1)}(q^2) \right) - q^\mu q^\nu \Pi_{A,3}^{(0)}(q^2), \end{aligned} \quad (3.23)$$

where $\Pi_{V,3}^{(1)}$, $\Pi_{A,3}^{(1)}$ and $\Pi_{A,3}^{(0)}$ are respectively the spin-one and spin-zero correlators. The spectral functions are proportional to the imaginary parts of the corresponding correlators,

$$\mathcal{Im} \Pi_{V/A,3}^{(1)}(s) = \pi \rho_{V/A,3}(s) \quad \mathcal{Im} \Pi_{A,3}^{(0)}(s) = \pi \rho_{A,3}^{(0)}(s). \quad (3.24)$$

They encode how the isospin vector and axial-vector currents excite various n -pion states at invariant energy $s < m_\tau^2$. Figure V–2 displays the $V - A$ spectral function⁸ $(\rho_{V,3} - \rho_{A,3})(s)$ as measured in tau decay from the ALEPH collaboration. The first peak is from the ρ meson, followed by the negative a_1 peak and then the four-pion component, etc.

Some applications of τ decays

Studies of τ decays have also proved valuable in providing a measure of $\alpha_s(m_\tau)$. Such a determination is significant because the tau lepton mass is one of the lowest energy scales (the charm quark mass is another) at which this is possible. The procedure essentially amounts to performing a more careful evaluation of R_τ than

⁸ Here and henceforth we abbreviate $\rho_{V,3} \rightarrow \rho_V$ and $\rho_{A,3} \rightarrow \rho_A$.

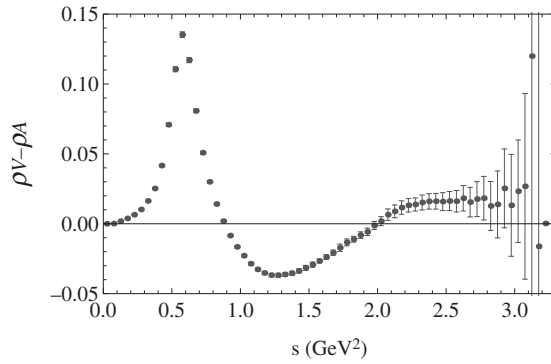


Fig. V-2 Authors' representation of ALEPH data for the $V - A$ spectral functions from tau decay.

the naive reasoning leading to the result in Eq. (3.5). Recall that we have previously displayed in Eq. (3.3) the measured value of R_τ . If we restrict ourselves to the Cabibbo-allowed decays (notationally, $R_\tau \rightarrow R_\tau^{\text{ud}}$) by subtracting off the Cabibbo suppressed transitions, then experiment gives [Pi 13]

$$R_\tau^{\text{ud}} = 3.4771 \pm 0.0084. \tag{3.25a}$$

On the theory side, a careful analysis of tau decays yields

$$R_\tau^{\text{ud}} = N_C |V_{\text{ud}}|^2 S_{\text{EW}} [1 + \delta_{\text{NP}} + \delta_{\text{P}}], \tag{3.25b}$$

where S_{EW} is an electroweak correction,

$$S_{\text{EW}} = 1 + \frac{2\alpha(m_\tau)}{\pi} \ln\left(\frac{M_Z}{m_\tau}\right) + \dots = 1.0201 \pm 0.0003 \tag{3.25c}$$

and $\delta_{\text{NP}} \simeq -0.0059 \pm 0.0014$ represents the nonperturbative QCD corrections. These two are insignificant compared to δ_{P} , the perturbative QCD correction, whose numerical value is inferred by comparing the above experimental and theoretical relations,

$$\delta_{\text{P}} = 0.2030 \pm 0.0033, \tag{3.25d}$$

amounting to a 20% effect. To derive a theoretical expression for δ_{P} , one first expresses R_τ^{ud} as the contour integral [BrNP 92]

$$R_\tau^{\text{ud}} = 6\pi i \oint_{|s|=m_\tau^2} \frac{ds}{m_\tau^2} \left(1 - \frac{s}{m_\tau^2}\right)^2 \times \left[\left(1 + 2\frac{s}{m_\tau^2}\right) \Pi^{(1+0)}(s) - 2\frac{s}{m_\tau^2} \Pi^{(0)}(s) \right], \tag{3.26}$$

where the presence of $\Pi^{(1+0)}$ in the above is associated with requiring singularity-free behavior in the complex- q^2 plane upon passing to the chiral limit. We shall not detail the next steps, which involve use of the operator-product expansion (OPE) for $\Pi^{(1+0)}(s)$ on the circle $|s| = m_\tau^2$. However, the physical picture which emerges is akin to that of the quark–antiquark loop in electromagnetic vacuum polarization (cf. Fig. II–2(a)), except now the currents are the weak currents, and the photon-exchange perturbations of the EM case become instead gluon exchanges. The result of this is expressed as the series

$$\delta_P = \sum_{n=1} K_n A^{(n)}(\alpha_s) \tag{3.27a}$$

where $K_1 = 1$, $K_2 = 1.63982$, etc., and

$$A^{(n)}(\alpha_s) = \frac{1}{2\pi i} \oint_{|s|=m_\tau^2} \frac{ds}{s} \left(\frac{\alpha_s(-s)}{\pi} \right)^n \left(1 - 2\frac{s}{m_\tau^2} + 2\frac{s^3}{m_\tau^6} - \frac{s^4}{m_\tau^8} \right). \tag{3.27b}$$

The $\alpha_s(-s)$ dependence is expressible in terms of $\alpha_s(m_\tau)$, which finally can be determined in terms of the experimentally measured R_τ^{ud} . Depending on details of the analysis, some scatter occurs in the value found for $\alpha_s(m_\tau^2)$. The averaging in [Pi 13] (see also [Bo *et al.* 12]) arrives at

$$\alpha_s(m_\tau^2) = 0.334 \pm 0.014, \tag{3.28}$$

having about 4% uncertainty. Renormalization group running of this result up to the Z-boson mass gives $\alpha_s(M_Z) = 0.1204 \pm 0.0016$, in accord with the 2011 world average value $\alpha_s(M_Z) = 0.1183 \pm 0.0010$.

A rather different bit of τ -related physics involves a set of sum rules which contain the $\rho_{V,A}$ spectral functions [We 67a; Das *et al.* 67],

$$\int_{m_\pi^2}^\infty ds \frac{\rho_V(s) - \rho_A(s)}{s} = -4L'_{10}(\mu) + \frac{1}{16\pi^2} \ln \left(\frac{m_\pi^2}{\mu^2} \right), \tag{3.29a}$$

where $L'_{10}(\mu)$ is a chiral coefficient to be defined in Sect. VII–2 and quantified in Table VII–1, and μ is an arbitrary energy scale which cancels between the two terms on the right-hand side,

$$\int_{m_\pi^2}^\infty ds (\rho_V(s) - \rho_A(s)) = F_\pi^2, \tag{3.29b}$$

$$\int_0^\infty ds s (\rho_V(s) - \rho_A(s)) = 0, \tag{3.29c}$$

$$\int_0^\infty ds s \ln \left(\frac{s}{\Lambda^2} \right) (\rho_V(s) - \rho_A(s)) = -\frac{16\pi^2 F_\pi^2}{3e^2} (m_{\pi^\pm}^2 - m_{\pi^0}^2), \tag{3.29d}$$

where Λ is an energy scale which is arbitrary by virtue of Eq. (3.29c). Although the sum rules of Eqs. (3.29a,b) hold in the physical world, those of Eqs. (3.29c,d) are derived in the chiral limit of massless u, d quarks, so the quantities F_π and m_{π^\pm} are understood to have slightly different numerical values from their physical counterparts. Like the extraction of $\alpha_s(m_\tau)$ from τ decay, these sum rules have been the subject of much study over time. Their convergence is sensitive to the spectral functions in the large s limit. This is known in the $m_u = m_d$ limit to be $(\rho_{V,3} - \rho_{A,3})(s) \sim s^{-3}$, which suffices to provide convergence.

Another, perhaps surprising, application of the spectral functions $\rho_{V,3}$ and $\rho_{A,3}$ involves CP violation in the kaon system. This is presented in Sect. IX–3, where the association of these spectral functions with ϵ'/ϵ (a measure of direct to indirect CP violation) is described.

Problems

(1) Effective lagrangian for $\mu \rightarrow e + \gamma$

In describing the decay $\mu \rightarrow e + \gamma$, one may try to use an effective lagrangian $\mathcal{L}_{3,4}$ which contains terms of dimensions 3 and 4,

$$\mathcal{L}_{3,4} = a_3 (\bar{e}\mu + \bar{\mu}e) + ia_4 (\bar{e}\not{D}\mu + \bar{\mu}\not{D}e),$$

where $D_\mu \equiv \partial_\mu + ieQ_{el}A_\mu$ and a_3, a_4 are constants.

- (a) Show by direct calculation that $\mathcal{L}_{3,4}$ does *not* lead to $\mu \rightarrow e + \gamma$.
- (b) If $\mathcal{L}_{3,4}$ is added to the QED lagrangian for muons and electrons, show that one can define new fields μ' and e' to yield a lagrangian which is diagonal in flavor. Thus, even in the presence of $\mathcal{L}_{3,4}$, there are *two* conserved fermion numbers.
- (c) At dimension 5, $\mu \rightarrow e + \gamma$ can be described by a gauge-invariant effective lagrangian containing constants c, d ,

$$\mathcal{L}_5 = \bar{e}\sigma^{\alpha\beta}(c + d\gamma_5)\mu F_{\alpha\beta} + \text{h.c.}$$

Obtain bounds on c, d from the present limit for $\mu \rightarrow e + \gamma$.

(2) Muon decay

- (a) Obtain the leading $\mathcal{O}(m_e^2/m_\mu^2)$ correction to the Fermi-model expression Eq. (2.10) for the muon decay width.
- (b) Do the same for the leading $\mathcal{O}(m_\mu^2/M_W^2)$ correction.

(3) Vacuum polarization and dispersion relations

The vacuum polarization $\Pi(q^2)$ associated with a loop containing a spin one-half fermion–antifermion pair, each of mass m , can be written as the sum of a term containing an ultraviolet cut-off Λ and a finite contribution $\hat{\Pi}_f(q^2)$,

$$\begin{aligned}\Pi(q^2) &= \frac{\alpha}{\pi} \left[\frac{1}{3} \ln \frac{\Lambda^2}{m^2} - 2 \int_0^1 dx x(1-x) \ln \left(1 - \frac{q^2}{m^2} x(1-x) \right) \right] \\ &\equiv \frac{\alpha}{3\pi} \ln \frac{\Lambda^2}{m^2} + \hat{\Pi}_f(q^2).\end{aligned}$$

- (a) Show that $\hat{\Pi}_f(q^2)$ is an analytic function of q^2 with branch point at $q^2 = 4m^2$ and with $\text{Im } \hat{\Pi}_f(q^2) = \alpha R_f(q^2)/3$, where

$$R_f(q^2) \equiv \sqrt{\frac{q^2 - 4m^2}{q^2}} \frac{2m^2 + q^2}{q^2}$$

is related to the rate for radiative pair creation via

$$\sum_f (2\pi)^3 \delta^{(4)}(q - p_f) \langle f | J_{\text{em}}^\nu | 0 \rangle^* \langle f | J_{\text{em}}^\mu | 0 \rangle = (-q^2 g^{\mu\nu} + q^\mu q^\nu) \frac{R_f(q^2)}{3}.$$

- (b) Use Cauchy's theorem and the result of (a) to express

$$\hat{\Pi}_f(q^2) = \frac{\alpha q^2}{3\pi} \int_{4m^2}^{\infty} ds \frac{R_f(s)}{s(s - q^2 - i\epsilon)}.$$

- (c) The form of $\hat{\Pi}_f(q^2)$ given in part (a) can be re-expressed in a dispersion representation. First change variables in (a) to $y = 1 - 2x$ and integrate by parts to obtain

$$\begin{aligned}\hat{\Pi}_f(q^2) &= -\frac{\alpha}{2\pi} \int_0^1 dy \ln \left[1 - \frac{q^2(1-y^2)}{4m^2 - i\epsilon} \right] \frac{d}{dy} \left(y - \frac{1}{3}y^3 \right) \\ &= \frac{\alpha}{2\pi} \int_0^1 dy 2y \left(y - \frac{y^3}{3} \right) \frac{q^2}{4m^2 - q^2(1-y^2) - i\epsilon}.\end{aligned}$$

Then, change variables again to $s = 4m^2/(1 - y^2)$ and demonstrate that the dispersion result of (b) obtains.